Dear author,

Please note that changes made in the online proofing system will be added to the article before publication but are not reflected in this PDF.

We also ask that this file not be used for submitting corrections.

Original Article

Inhibition of microRNA-222 expression accelerates bone healing with enhancement of osteogenesis, chondrogenesis, and angiogenesis in a rat refractory fracture model

Q2 Masaaki Yoshizuka [a, *], Tomoyuki Nakasa [a], Yoshitaka Kawanishi [a], Susumu Hachisuka [a], Taisuke Furuta [a], Shigeru Miyaki [b], Nobuo Adachi [a], Mitsuo Ochi [a]

[a] Department of Orthopedic Surgery, Graduate School of Biomedical Sciences, Hiroshima University, Hiroshima, Japan
[b] Department of Regenerative Medicine, Hiroshima University Hospital, Japan

ARTICLE INFO

ABSTRACT

Background: It is difficult to achieve bone union in case of non-union with non-invasive techniques. MicroRNAs (miRNAs) are short, non-coding RNAs that act as repressors of gene expression at the level of post-transcriptional regulation. This study focuses on microRNA (miR)-222 as it is known to be a negative modulator of angiogenesis, an essential component of fracture healing. The purpose of this study was to analyze the effects of miR-222 on osteogenic and chondrogenic differentiation in human mesenchymal stromal cell (MSC)s *in vitro*, and to determine whether local administration of miR-222 inhibitor into the fracture site could achieve bone union *in vivo*.
Method: miR-222 expression in human bone marrow mesenchymal stem cells (hMSCs), and osteogenic differentiation in hMSCs, were investigated. The gain or loss of miR-222 function was examined, in order to assess the effects of miR-222 on osteogenic and chondrogenic differentiation in hMSCs. A femoral transverse fracture was completed in rats, and the periosteum at the fracture site was cauterized. Then, either an miR-222 inhibitor or an miR-222 mimics, mixed with atelocollagen, was administered into the fracture site. A non-functional inhibitor negative control was administered to the control group. At 2, 4, 6, and 8 weeks, radiographs of the fractured femurs were obtained. Immunohistochemistry was performed at 2 weeks to evaluate the capillary density. At 8 weeks, micro-computed tomography (μCT) imaging analysis and histological evaluations were performed.
Results: The expression of miR-222 significantly decreased as osteogenic differentiation of hMSCs proceeded. Inhibition of miR-222 promoted osteogenic differentiation, and over expression of miR-222 inhibited osteogenic differentiation in hMSCs, which was confirmed by measuring expression of Runx2, collagen type 1A1 (COL1A1), and osteocalcin. Inhibition of miR-222 promoted chondrogenic differentiation in hMSCs, which was confirmed by measuring expression of collagen type II (COL2A1), aggrican, and SOX9. Bone union at the fracture site was achieved in only the groups treated with the miR-222 inhibitor, confirmed by radiographic, μCT and histological evaluation at 8 weeks after administration. Immunohistochemistry showed that capillary density in the miR-222 inhibitor group was significantly higher than that in the control group and in the miR-222 mimics group.
Conclusion: Local administration of miR-222 inhibitor can accelerate bone healing by enhancing osteogenesis, chondrogenesis, and angiogenesis in the rat refractory model.

1. Introduction

Although a bone fracture heals without any special treatment under optimal conditions, in some situations it can fail to achieve bone union, with additional treatment required to induce bone formation [1]. It is still difficult to achieve bone union in cases of non-union in a clinical setting, and bone-grafting is set as the

* Corresponding author. Department of Orthopedic Surgery, Graduate School of Biomedical Sciences, Hiroshima University, Hiroshima, 1-2-3, Kasumi, Minami-Ku, Hiroshima, 734-8551, Japan. Fax: +81 822575234.
   E-mail address: yoshizukamasaaki@yahoo.co.jp (M. Yoshizuka).

treatment gold standard for such cases. However, the disadvantages of bone grafting include the risk of infection, hematoma/seroma, further bone fracture, nerve and vascular injuries, residual pain, unsightly scars and poor cosmetic outcomes at the donor site [2]. Therefore, the development of new, effective therapeutic strategies with minimal invasion for case of non-union is desirable.

MicroRNAs (miRNAs) are short, non-coding RNAs that act as repressors of gene expression at the level of post transcriptional regulation [3]. MiRNAs bind to the 3′-UTR region of mRNA of target genes, and induce mRNA degradation or inhibit protein translation, subsequently regulating gene expression. Overexpression or downregulation of miRNAs can simultaneously regulate the endogenous expression of multiple growth factors [4]. Previous studies have reported on the use of miRNA inhibitors or mimics, including miR-26a, miR-31 and miR-92a, for bone regeneration in *in vivo* experiments, successfully accelerating bone formation with this less invasive procedure [5–7]. However, there have been no reports of local administration of miRNA inhibitors or mimics into the fracture site in the refractory fracture model. Several studies have suggested that miR-222 plays an important role in vascular formation [8,9], which is an essential part of fracture healing [10]. In this study, we analyzed the effects of miR-222 on osteogenic and chondrogenic differentiation in human mesenchymal stromal cell (MSC)s *in vitro*, and investigated whether local administration of an miR-222 inhibitor into the fracture site could achieve bone union *in vivo*.

2. Materials and methods

2.1. In vitro experiments

2.1.1. Cell culture

Human bone marrow derived MSCs (LONZA, Basel, Switzerland) from 5 donors (Lot Number:0000296577, 0000310956, 0000318006, 0000296578, 0000307219) were cultured in human MSC culture medium (StemPro MSC SFM, Invitrogen, Carlsbad, USA) with antibiotics in humidified air containing 5% CO_2 at 37 °C.

2.1.2. Transfection of miR-222 mimics and inhibitor into MSCs

In total, 2×10^4 hMSCs were seeded in 24-well plates overnight, after which the medium was changed to osteogenic medium (StemPro Osteogenesis Differentiation Kit, Invitrogen). One day after osteogenesis induction, the miR-222 inhibitor (Qiagen, Hilden, Germany) or a non-functional inhibitor negative control (Qiagen), and miR-222 mimics (BIONEER, Almeda, CA, USA) or non-functional negative control miRNA (BIONEER) were transfected into MSCs using Lipofectamine-RNAi MAX (Invitrogen) following the manufacturer's instructions. The transfection reagent was diluted in Opti-MEM1 (Invitrogen) and mixed with 100 nM miR-222 inhibitor, 50 nM miR-222 mimics, or with the same concentrations of the negative controls. After incubating for 10 min at room temperature, the mixture was dispensed into 24-well plates and cultured in an incubator with humidified air containing 5% CO_2 at 37 °C. At 6 h after transfection, the medium was replaced by a new osteogenic medium. To examine the roles of miR-222 in chondrogenic differentiation in hMSCs, hMSCs were transfected with the miR-222 inhibitor or the inhibitor negative control or the miR-222 mimics or negative control miRNA, using Lipofectamine-RNAi MAX in the same manner described as above. At 6 h after transfection, the transfected hMSCs were trypsinized. To form pellet cultures, 2.5×10^5 hMSCs were centrifuged (1200 rpm, 5 min) in a 15 mL Falcon Tube (Corning, NY, USA). Cells were cultured under chondrogenic conditions for 14 days in differentiation medium (Differentiation Basal Medium-Chondrogenic, LONZA) with 1% antibiotic-antimycotic solution,

37 nM BMP2 (Wako Pure Chemical Industries, Ltd. Osaka Japan) and 0.79 nM TGF-b3 (Wako Pure Chemical Industries, Ltd.) according to a previously described protocol [11]. The pellet medium was changed every 3 days, and cell pellets were cultured for 14 days with chondrogenic medium prior to analysis.

2.1.3. Quantitative real time polymerase chain reaction

Cells were harvested and total RNA was isolated from cells using TRIzol (GIBCO BRL, Palo Alto, CA, USA) according to the manufacturer's instructions. Quantitative PCR assays were performed with a TaqMan miRNA assay kit (Applied Biosystems, Foster City, CA, USA) for miR-222 and snRNAU6, and TaqMan mRNA assay kit for the Runx2, collagen type 1A1 (COL1A1), osteocalcin, collagen type II (COL2A1), aggrecan, SOX9 and GAPDH. Total RNA (10 ng) was reverse transcribed using the TaqMan MicroRNA Reverse Transcription Kit for miR-222. Furthermore, total RNA (1 μg) was reverse transcribed using the super script VIVO master mix (Invitrogen) for mRNA. Quantitative real time PCR was performed using a TaqMan Fast Advanced PCR Master Mix (Applied Biosystems, Foster City, CA, USA) in combination with a StepOne and Biosystems Real-time PCR System (Applied Biosystems) for both miR-222 and mRNA. Expression of miR-222 was evaluated at 3, 7, and 14 days after osteogenic differentiation of MSCs relative to native hMSCs. Expression of miR-222 was evaluated at post-transfection day 1, Runx2 and COL1A1 at post-transfection day 5, and osteocalcin at post-transfection day 10 in the miR-222 inhibitor group and miR-222 mimics group, relative to the miR-222 inhibitor control group and miR-222 mimics control group, respectively. Expression of COL2A1, aggrecan, and SOX9 was evaluated at post-transfection day 14 after chondrogenic differentiation of hMSCs in the miR-222 inhibitor group and miR-222 mimics group, relative to the miR-222 inhibitor control group and miR-222 mimics control group, respectively. The expression of miR-222 was assessed relative to the expression of snRNAU6, and the expression of other genes was assessed relative to the expression of GAPDH. A threshold cycle (Ct) was observed in the exponential phase of amplification, and quantification of the relative expression levels was performed using standard curves for the target genes and for the endogenous controls. Geometric means were used to calculate the delta−delta Ct ($\Delta\Delta$Ct) values and were expressed as $2^{-\Delta\Delta C_t}$. Each control sample was set to a value of 1, and the fold-change of the target genes was calculated with this value as a reference.

2.1.4. Alkaline phosphatase activity

An analysis of alkaline phosphatase (ALP) activity was performed 10 days after transfection. Washed with distilled water, total protein then was desorbed with 150 μL of 0.3% Triton X for 3 min. This solution was homogenized, then ALP activity was assayed by a spectrophotometric measurement of p-nitrophenol release at 37 °C using a Labo assay TM ALP (Wako Pure Chemical Industries, Ltd. Osaka Japan). Finally, the ALP levels were normalized according to the total protein content.

2.1.5. Alizarin red staining

For detection of calcification during differentiation, 14 days after transfection, cells were fixed with 4% paraformaldehyde (PFA) for 15 min, washed with distilled water, stained with 1% Alizarin red staining solution for 20 min, and then washed again to remove excess dye. Images of the cells were acquired using a microscope.

2.2. In vivo experiments

2.2.1. Animal model

Twelve-week-old male adult Sprague Dawley (SD) rats (CLEA Japan, Inc. Tokyo, Japan) were used in this study. The rat femoral

refractory fracture model was built using a modified version of a previously published method [12]. All surgical procedures were performed under normal sterile conditions and animals were anesthetized by intraperitoneal administration of sodium 5-ethyl-5-barbiturate. A lateral parapatellar incision was made to expose the distal femoral condyle. A 1.2-mm diameter Kirschner-wire was inserted from the trochlear groove into the femoral canal in a retrograde manner. The vastus muscle was divided longitudinally and the femur isolated. A thin saw cut at a depth of 3 mm was applied to the mid-shaft to weaken the bone, and a transverse femoral shaft fracture was completed manually. After this procedure, the periosteum at the fracture site was cauterized at a distance of 2 mm on each side of the fracture. Immediately after inducing the fracture, the rats were divided into 3 groups; 1) the miR-222 inhibitor group (n = 9), where the miR-222 inhibitor mixed with atelocollagen (Koken, Tokyo, Japan) was administrated into the surrounding area of the fracture site under direct vision; 2) the control group (n = 9), which were administrated with the inhibitor negative control; 3) the miR-222 mimics group (n = 9), which were administered with the miR-222 mimics. The miR-222 inhibitor (sequences 5′-UCAGUAGCCAGUGUAGAUCCU-3′) and atelocollagen complex was prepared as follows: 30 μL of atelocollagen and 30 μL of miR-222 inhibitor solution (miR-222 inhibitor 50 μg; buffer 3 μL; sterilized water 27 μL) was combined and mixed by rotation at 4 °C for 20 min. The inhibitor negative control and miR-222 mimics (sequences 5′-CUCAGUAGCCAGUGUAGAUCCU-3′) and atelocollagen complex were also prepared in the same manner. The wound was then closed in layers. Unprotected weight bearing was allowed immediately for both groups. For the purpose of histological evaluation, all rats were sacrificed by terminal anesthesia at 2 (n = 4 in each group) and 8 (n = 5 in each group) weeks.

2.2.2. Radiographic evaluation

Radiographs of the fractured femurs were serially obtained at 2, 4, 6, and 8 weeks after administration of the miR-222 inhibitor, inhibitor negative control, or the miR-222 mimics, with the anesthetized animal in a supine position (n = 5 in each group). Radiographic images were graded using the previously defined scale of Murata et al. [7]. The radiographic scoring system was as follows: 1, no apparent hard callus; 2, slight intramembranous ossification; 3, hard callus without bridging of the fracture gap, and fracture line apparent; 4, hard callus with bridging of the fracture gap, and fracture gap noticeable; 5, unclear boundary between the newly hard callus and existing cortical bone; 6, remodeling. To determine whether the bone union was complete, micro-computed tomography (μCT) imaging analysis was performed at 8 weeks after administration using the SkyScan1176 (TOYO Corporation, Tokyo, Japan). After the μCT scan, 3-dimensional CT images were reconstructed using CT Analysis Software placed on the main torso (NRecon and CTvox). The diagnosis of bone union was based on the presence of bridging bone at the fracture site and the disappearance of the fracture line. The radiographic scoring and the diagnosis of bone union was analyzed by 3 orthopedic surgeons (not authors) who were blinded to the treatment.

2.2.3. Tissue harvesting and histological analysis

Rat femurs were harvested and then fixed with 4.0% PFA at 4 °C for 24 h. Tissue samples were decalcified with 100% KCX (Falma, Osaka, Japan) at 4 °C for 3 days. The specimens were dehydrated through an ethanol and xylene series and embedded in paraffin before being sectioned (6 μm slices) along the longitudinal axis of the femur with a microtome. Histological evaluations (n = 5 in each group) were performed using toluidine blue staining to address the degree of fracture healing at 8 weeks after administration. Sections were analyzed using a digital microscope (BZ-9000, Keyence,

Osaka, Japan). The degree of fracture healing was evaluated using the ten-point scale proposed by Oetgen et al. [13]. The scoring system for fracture healing was as follows: 1, fibrous tissue; 2, predominantly fibrous tissue with a small amount of cartilage; 3, equal mixture of fibrous and cartilaginous tissue; 4, predominantly cartilage with a small amount of fibrous tissue; 5, cartilage; 6, predominantly cartilage with a small amount of immature bone; 7, equal mixture of a small amount of cartilage and immature bone; 8, predominantly immature bone with a small amount of cartilage; 9, union of immature bone fracture fragments; 10, union of mature bone fracture fragments. The histological scoring was analyzed by 3 orthopedic surgeons (not authors) who were blinded to the treatment.

2.2.4. Evaluation of capillary density at fracture sites

Samples (n = 4 in each group) were harvested 2 weeks after administration, fixed in 4% PFA and then decalcified with 5% EDTA for 3 weeks, followed by paraffin embedding. The paraffin-embedded 6 μm serial sections were stained with fluorescein-labeled GSL I-isolectin B4 (Vector Laboratories, Burlingame, CA, USA). In order to evaluate newly formed vessels, 5 microscopic areas (500 × 600 μm) in the fracture callus from each specimen at 200× magnification were randomly chosen. Capillaries were recognized as tubular structures positive for isolectin B4, and the number of capillaries was counted.

The evaluation was analyzed by 3 orthopedic surgeons (not authors) who were blinded to the treatment.

2.2.5. Statistical analyses

All results in this study were expressed as the mean ± S.E. A comparison of miR-222 expression during the osteogenic differentiation of hMSCs was made using one-way ANOVA followed by the Tukey−Kramer test. The paired t test was used for the comparison between the miR-222 inhibitor groups or miR-222 mimic groups, and the corresponding control groups in the in vitro study. Differences between 3 groups were analyzed using one-way ANOVA followed by the Tukey−Kramer test in the in vivo study. A probability value of less than 0.05 was considered statistically significant.

3. Results

3.1. In vitro experiments

3.1.1. Roles of miR-222 during osteogenic differentiation in hMSCs

To clarify the expression pattern of miR-222 during osteogenesis, the expression levels of miR-222 were analyzed at each time point during the osteogenic differentiation in hMSCs by real-time PCR. The miR-222 expression at days 7 and 14 was significantly down-regulated compared to the native hMSCs (n = 5, $p < 0.05$), suggesting that miR-222 participates in osteogenic differentiation in hMSCs (Fig. 1A). The intracellular level of miR-222 in hMSCs was significantly reduced by the transfection of the miR-222 inhibitor (n = 5, $p < 0.05$) and significantly elevated by the transfection of the miR-222 mimics (n = 5, $p < 0.05$) at 1 day after transfection (Fig. 1B, C). The expression of 3 osteogenic markers, Runx2, COL1A1 at post-transfection day 5, and osteocalcin at post-transfection day 10, was analyzed. Inhibition of miR-222 significantly up-regulated the expression levels of Runx2, COL1A1 and osteocalcin (n = 5, $p < 0.05$ respectively). In contrast, overexpression of miR-222 significantly downregulated the expression of these genes (n = 5, $p < 0.05$ respectively) (Fig. 2A−C). ALP activity was significantly increased on day 10 after transfection of inhibitor miR-222 (n = 5, $p < 0.05$), while it was significantly decreased by the transfection of the miR-222 mimics (n = 5, $p < 0.05$) (Fig. 2D). On day 14 after transfection, Alizarin red staining was enhanced in
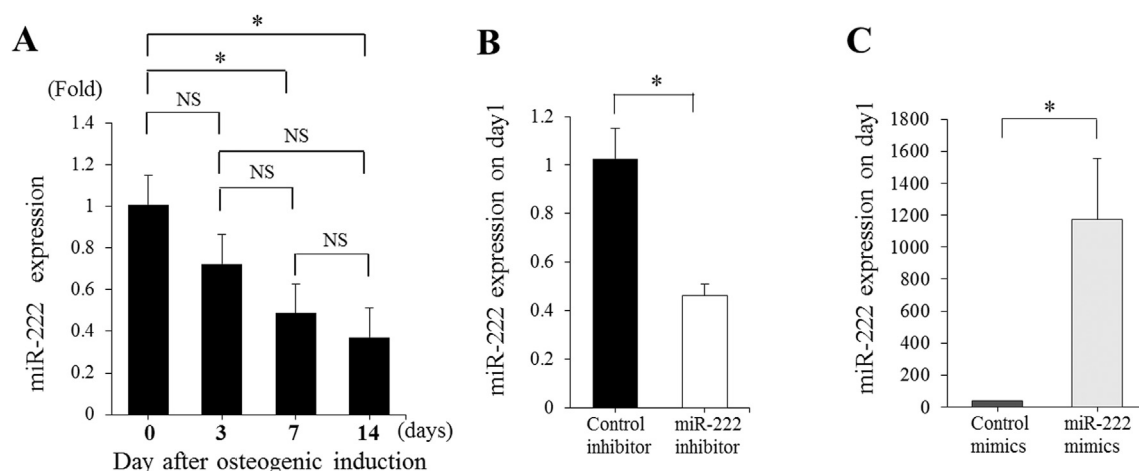
Fig. 1. Expression of miR-222 was analyzed at each time point during osteogenic differentiation in MSCs by real-time PCR (n = 5 in each group) (A). Expression of miR-222 at one day after the miR-222 inhibitor transfection (B) and expression of miR-222 at one day after the miR-222 mimics transfection (n = 4 in each group) (C). *p < 0.05 in the indicated group. *NS*, no significant difference in the indicated group.
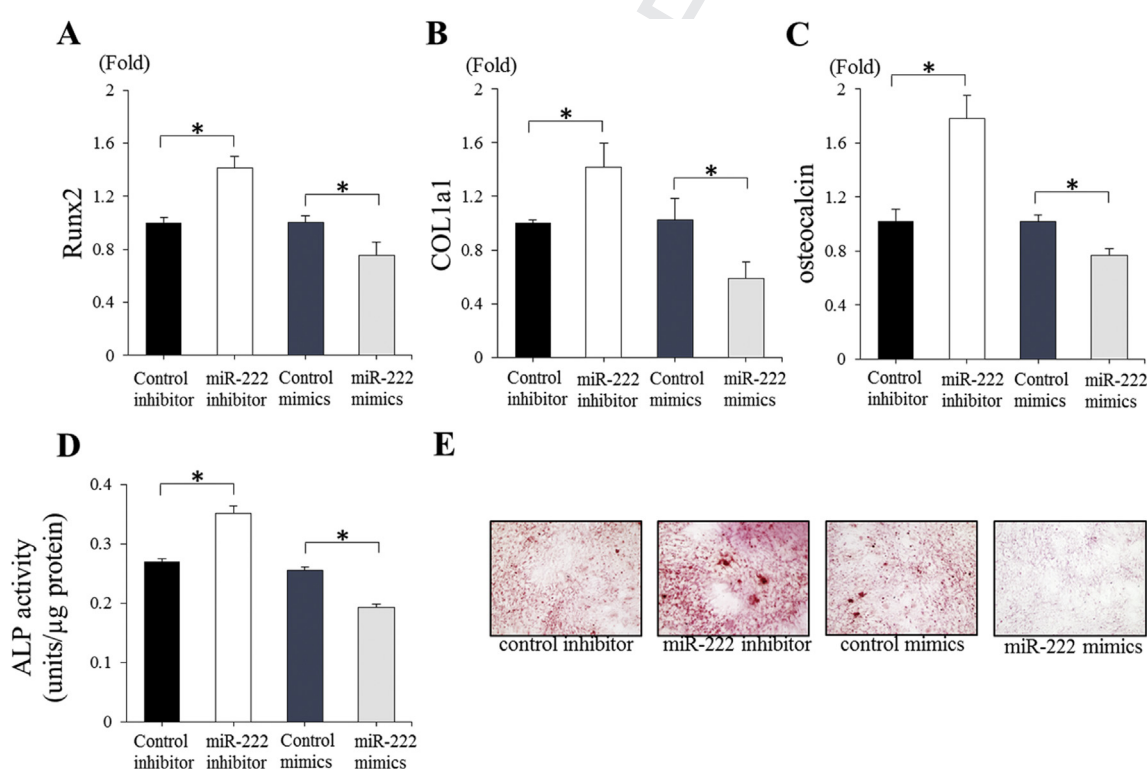

Fig. 2. Real-time PCR analysis of Runx2 (A) and COL1A1 (B) at 5 days and osteocalcin (C) at 10 days after transfection (n = 5 in each group). ALP activity on day 10 after transfection (n = 5 in each group) (D). Alizarin red staining at 14 days after transfection (original magnification, ×40) (E). COL1a1, collagen type 1A1. ALP, Alkaline phosphatase activity. *p < 0.05 in the indicated group.

groups transfected with the miR-222 inhibitor, compared to groups transfected with the miR-222 mimics or negative control groups (Fig. 2E). Taken together, our results suggest that miR-222 is a negative regulator of osteoblast differentiation in hMSCs.

3.1.2. Role of miR-222 during chondrogenic differentiation in hMSCs

To analyze the effects of miR-222 on chondrogenic differentiation, we analyzed the expression of COL2A1, aggrecan, and SOX9 at post-transfection day 14. Inhibition of miR-222 significantly upregulated the expression of these genes (n = 5, p < 0.05 respectively)

(Fig. 3A–C). No significant differences in the expression of these genes were observed between the mimics control and the miR-222 mimics groups (Fig. 3A–C). These results indicate that inhibition of miR-222 promotes chondrogenic differentiation in hMSCs.

3.2. In vivo experiments

3.2.1. Local administration of miR-222 inhibitor enhanced fracture healing of the femur

All femurs in the miR-222 inhibitor group showed bone union at 8 weeks after administration of the treatment by the confirmed
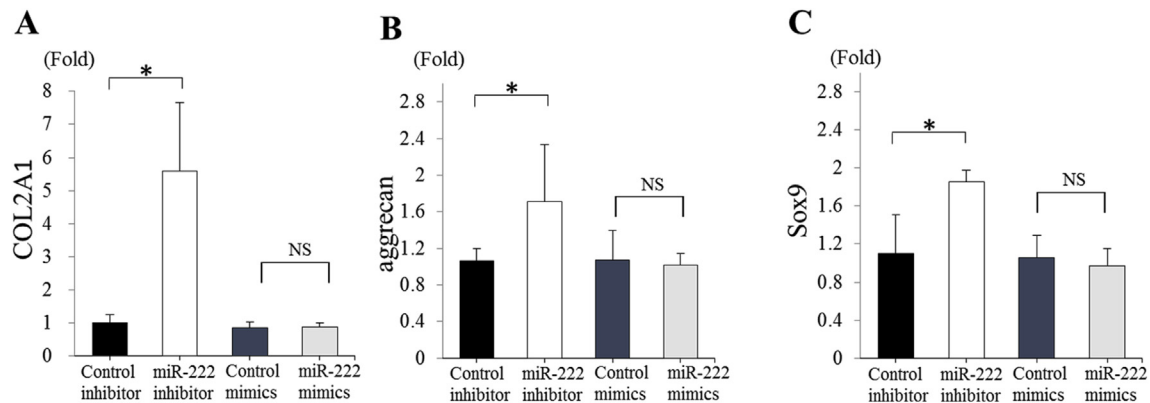
Fig. 3. Real-time PCR analysis of COL2A1 (A), SOX9 (B) and aggrecan (C) at 14 days after transfection (n = 5 in each group). COL2A1; Collagen type II. *p < 0.05 in the indicated group. *NS*, no significant difference in the indicated group.

disappearance of the fracture line on X-ray photography (XP) and μCT images. No femurs in the control group or the miR-222 mimics group showed bone union. The control group and the miR-222 mimic group showed some extent of callus formation, but the fracture line remained (Fig. 4A, B).

At 8 weeks after administration, the mean radiological score in the control group was 3.6 ± 0.24, which was significantly lower than that in the miR-222 inhibitor group, (5 ± 0) and higher than that in the miR-222 mimic group (2.6 ± 0.22) (p < 0.05, n = 5 in each group). Histological analysis of specimens at 8 weeks revealed that the fracture in the miR-222 inhibitor group was bridged by woven bone at the fracture site; this was not found in the control group and the fracture site was filled with cartilage tissue, while in the miR-222 mimics group, the fracture site was filled with fibrous and cartilage tissue (Fig. 5A). At 8 weeks, the mean fracture healing scores of histological evaluation were 5.4 ± 0.24, 8.2 ± 0.2, and 4 ± 0.32 for the control, miR-222 inhibitor, and miR-222 mimics groups, respectively. There were significant differences among the
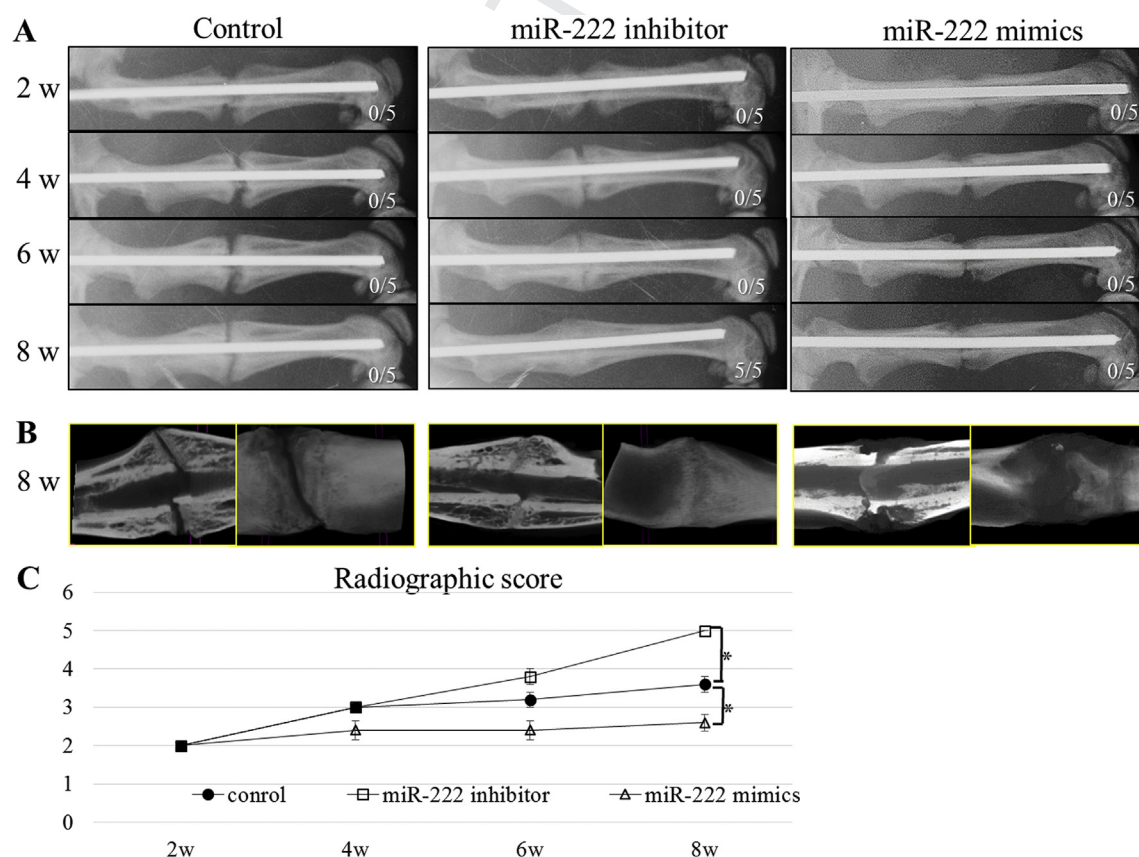

Fig. 4. Radiogram (A) at 2, 4, 6, and 8 weeks after surgery and μCT (B) at 8 weeks after surgery of the fracture in the control group, the miR-222 inhibitor group and the miR-222 mimics group. The radiographic score for the control group, the miR-222 inhibitor group and the miR-222 mimics group at 2, 4, 6 and 8 weeks after surgery (n = 5 in each group) (C). *p < 0.05 in the indicated group.
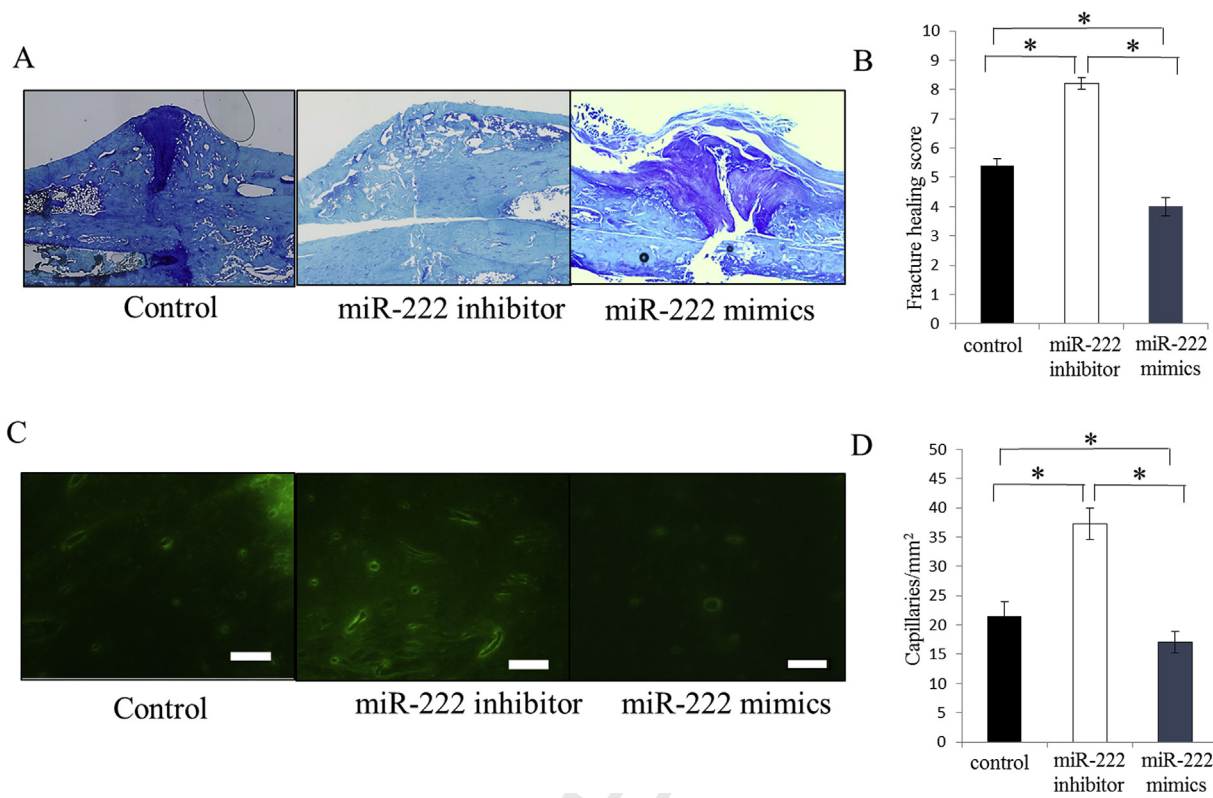
Fig. 5. (A) Histological evaluation using toluidine blue staining at 8 weeks after administration in the control group, the miR-222 inhibitor group and the miR-222 mimics group. (B) The mean fracture healing score for the control group, the miR-222 inhibitor group and the miR-222 mimics group at 8 weeks after surgery (n = 5 in each group). (C) Immunofluorescent analysis of isolectin B4 in both groups at 2 weeks after administration. The scale bar indicates 100 μm. (D) The capillary density in the control group, the miR-222 inhibitor group and the miR-222 mimics group at 2 weeks after surgery (n = 4 in each group). *p < 0.05 in the indicated group.

control group and the miR-222 inhibitor and miR-222 mimics groups (p < 0.05, n = 5 in each group) (Fig. 5B). Immunohistochemistry of isolectin B4 of specimens at 2 weeks showed that the capillary density was 21.4 ± 2.7/mm² in the control group, 37.5 ± 2.7/mm² in the miR-222 inhibitor group, and 17 ± 1.8/mm² in the miR-222 mimic group. There were significant differences among the control group and the miR-222 inhibitor and miR-222 mimic groups (p < 0.05, n = 4 in each group) (Fig. 5C, D). These results suggested that angiogenesis could be enhanced by the downregulation of miR-222, and decreased by the upregulation of miR-222 at the fracture site.

4. Discussion

This study has demonstrated that administration of an miR-222 inhibitor can enhance bone formation, even in the case of refractory fracture models in rats. A few studies have reported on the use of the miRNA inhibitors or mimics for bone regeneration in *in vivo* experiments. Li et al. reported that transfection of bone marrow MSCs with miR-26a mimics enables the complete repair of the critical size calvarial bone defect via enhancement of angiogenesis and osteogenesis [5]. Murata et al. reported that systemic and local administration of miR-92a enhanced fracture healing through angiogenesis in the mouse femoral fracture model [7]. Deng et al. reported that adipose tissue-derived stem cells knockdown miR-31, combined with beta-tricalcium phosphate scaffolds, were capable of repairing a rat critical-sized calvarial defect [6]. For the first time, the present study showed that local administration of an miR-222 inhibitor could accelerate bone healing through enhancing osteogenesis, chondrogenesis, and angiogenesis in the rat refractory fracture model.

Essential components of fracture healing comprise the appropriate development of blood vessels in the fracture callus [10], and the remodeling of calcified callus into woven bone by chondroclasts and osteoprogenitors [14]. From this point of view, the miR-222 inhibitor is an ideal agent to promote bone regeneration, since it can enhance osteogenesis, chondrogenesis, and angiogenesis. The current study has revealed that the expression of miR-222 in hMSCs is down-regulated during osteogenic differentiation. It has also revealed that inhibition of miR-222 in hMSCs after osteogenic induction significantly up-regulates the expression of Runx2, COL1A1, and osteocalcin. In contrast, overexpression of miR-222 in MSCs after osteogenic induction significantly downregulates the expression of these genes. Our results suggest that miR-222 is a negative regulator of osteogenic differentiation in hMSCs. MiRNAs simultaneously regulate the expression of multiple genes. A single miRNA can potentially target many mRNAs (an estimated range of one to several hundred), based on target predictions using the bioinformatics approach. Conversely, one mRNA can be influenced by several miRNAs [15]. Many target genes might interact to promote bone regeneration directly or indirectly via miR-222 inhibitors after local administration. Yu et al. used computational analysis to predict that miR-222 would have an inhibitory effect on genes associated with osteogenic differentiation, such as BMP2, osteocalcin, and Runx2 [16]. However, the target genes of miR-222 in osteogenic differentiation have not been validated. Hence, further research on this subject is required.

We also investigated the effects of miR-222 on chondrogenic differentiation in hMSCs, which is one of the essential components for endochondral ossification in secondary fracture healing [14], and demonstrated that the inhibitor of miR-222 induced an

increase of chondrogenic markers, including COL2A1, aggrecan, and SOX9 in hMSCs. The effect of the miR-222 inhibitor on chondrogenic differentiation was thought to be one of the factors leading to bone union.

In our *in vivo* experiment, immunohistochemistry of isolectin B4 showed that capillary density in the miR-222 inhibitor group was significantly higher than that in the control group, and that capillary density in the miR-222 mimic group was significantly lower than that in the control group. These results suggest that miR-222 is a negative regulator of angiogenesis. Several studies have suggested that miR-222 plays an important role in vascular formation. High levels of miR-222 expression were found in endothelial cells (ECs) and they were downregulated in ECs during neovascularization [8,9]. MiR-222 was found to negatively modulate angiogenesis by targeting the c-Kit receptor [8] together with the signal transducer and activator of transcription 5A (STAT5A) [9]. The c-Kit receptor is the receptor for the angiogenic activity of stem cell factor (SFC), and is expressed on the surface of ECs [8]. STAT5A activates bFGF and IL-3, which in turn trigger vascular EC morphogenesis in the STAT5A signaling pathway [9]. The present study demonstrated that although the target genes of miR-222 related to angiogenesis were not validated, down-regulation of the c-kit receptor and STAT5A by the miR-222 inhibitor might contribute to the enhanced neovascularization at the fracture site.

Delayed union and non-union are common complications following long-bone fracture, with a prevalence that ranges from 13% to 16%, depending on the location and severity of the injury to the bone and soft tissue [17]. For example, non-union of humeral shaft fractures often results in pain with prolonged disability resulting in reoperation, long extended from work, and impaired quality of life [18]. The success rate of the treatment of non-union is between 70% and 90% depending on the bone location and surgical method [19]. Therefore, a novel therapeutic strategy for non-union healing is clinically warranted. Waki et al. focused on the analysis of miRNA expression profiles in the non-union site of the rat femur, suggesting that miR-31a-3p, miR-31a-5p, miR-146a-5p, miR-146b-5p and miR-223-3p may play an important role in the development of non-union [20]. The study indicated that the therapeutic strategies using inhibitors of such miRNAs may be effective in treating non-union. Audige et al. documented that open tibia fractures with skin lesions have a greater risk of delayed healing or non-union than fractures with no skin injury [1]. In such cases, local administration to the fracture site of miR-222 inhibitor, as shown in the current study may prevent the development of delayed healing or non-union.

In conclusion, the present study has shown that local administration of miR-222 inhibitor into the fracture site is able to accelerate bone healing through enhancing osteogenesis, chondrogenesis, and angiogenesis in the rat refractory fracture model. To our knowledge, our results present the first evidence that a local administration of miRNA inhibitor/atelocollagen complexes may have therapeutic potential for refractory fractures.

Conflict of interest

The authors declare that they have no conflict of interest.

References

[1] Audige L, Griffin D, Bhandari M, Kellam J, Ruedi TP. Path analysis of factors for delayed healing and non-union in 416 operatively treated tibial shaft fractures. Clin Orthop Relat Res 2005 Sep;438:221–32.

[2] Dimitriou R, Mataliotakis GI, Angoules AG, Kanakaris NK, Giannoudis PV. Complications following autologous bone graft harvesting from the iliac crest and using the RIA: a systematic review. Injury 2011 Sep;42(2 suppl):3–15.

[3] Ambros V. The functions of animal microRNAs. Nature 2004 Sep;431(7006):350–5.

[4] Bartel DP. MicroRNAs: genomics, biogenesis, mechanism, and function. Cell 2004 Jan;116(2):281–97.

[5] Li Y, Fan L, Liu S, Liu W, Zhang H, Zhou T, Wu D, Yang P, Shen L, Chen J, Jin Y. The promotion of bone regeneration through positive regulation of angiogenic-osteogenic coupling using microRNA-26a. Biomaterials 2013 Jul;34(21):5048–58.

[6] Deng Y, Zhou H, Zou D, Xie Q, Bi X, Gu P, Fan X. The role of miR-31-modified adipose tissue-derived stem cells in repairing rat critical-sized calvarial defects. Biomaterials 2013 Sep;34(28):6717–28.

[7] Murata K, Ito H, Yoshitomi H, Yamamoto K, Fukuda A, Yoshikawa J, Furu M, Ishikawa M, Shibuya H, Matsuda S. Inhibition of miR-92a enhances fracture healing via promoting angiogenesis in a model of stabilized fracture in young mice. J Bone Min Res 2014 Feb;29(2):316–26.

[8] Poliseno L, Tuccoli A, Mariani L, Evangelista M, Citti L, Woods K, Mercatanti A, Hammond S, Rainaldi G. MicroRNAs modulate the angiogenic properties of HUVECs. Blood 2006 Nov;108(9):3068–71.

[9] Dentelli P, Rosso A, Orso F, Olgasi C, Taverna D, Brizzi MF. microRNA-222 controls neovascularization by regulating signal transducer and activator of transcription 5A expression. Arterioscler Thromb Vasc Biol 2010 Aug;30(8):1562–8.

[10] Hankenson KD, Dishowitz M, Gray C, Schenker M. Angiogenesis in bone regeneration. Injury 2011 Jun;42(6):556–61.

[11] Chen J, Li C, Wang S. Periodic heat shock accelerated the chondrogenic differentiation of human mesenchymal stem cells in pellet culture. PLoS One 2014 Mar;9:e91561.

[12] Kokubu T, Hak DJ, Hazelwood SJ, Reddi AH. Development of an atrophic nonunion model and comparison to a closed healing fracture in rat femur. J Orthop Res 2003 May;21(3):503–10.

[13] Oetgen ME, Merrell GA, Troiano NW, Horowitz MC, Kacena MA. Development of a femoral non-union model in the mouse. Injury 2008 Oct;39(10):1119–26.

[14] Bielby R, Jones E, McGonagle D. The role of mesenchymal stem cells in maintenance and repair of bone. Injury 2007 Mar;38(1 suppl):26–32.

[15] Didiano D, Hobert O. Perfect seed pairing is not a generally reliable predictor for miRNA-target interactions. Nat Struct Mol Biol 2006 Sep;13(9):849–51.

[16] Yu F, Cui Y, Zhou X, Zhang X, Han J. Osteogenic differentiation of human ligament fibroblasts induced by conditioned medium of osteoclast-like cells. Biosci Trends 2011 May;5(2):46–51.

[17] Sen MK, Miclau T. Autologous iliac crest bone graft: should it still be the gold standard for treating non-unions? Injury 2007 Mar;38(1 suppl):75–80.

[18] Dujardin FH, Mazirt N, Tobenas AC, Duparc F, Thomine JM. Failure of locked centro-medullary nailing in pseudarthrosis of the humeral diaphysis. Rev Chir Orthop Reparatrice Appar Mot 2000 Dec;86(8):773–80.

[19] Romano CL, Romano D, Logoluso N. Low-intensity pulsed ultrasound for the treatment of bone delayed union or non-union: a review. Ultrasound Med Biol 2009 Apr;35(4):529–36.

[20] Waki T, Lee SY, Niikura T, Iwakura T, Dogaki Y, Okumachi E, Kuroda R, Kurosaka M. Profiling microRNA expression in fracture non-unions: potential role of microRNAs in non-union formation studied in a rat model. Bone Jt J 2015 Aug;97-b(8):1144–51.